Our object of research is to combine the properties of Mn and the advantages of Fe-Al-C to improve the performance of grinding ball materials. Three Fe-5Al-1C alloys with compositions of 15 wt % Mn (FAM15), 20 wt % Mn (FAM20), and 25 wt % Mn (FAM25) were investigated. Argon gas was used to assist the removal of dissolved oxygen and to control the formation of metal oxides during Fe-Al-Mn-C (FAMC) fabrication. Microstructure analysis was conducted using scanning electron microscopy, and the Vickers microhardness tester was used to evaluate hardness. To guarantee the Fe-5Al-1C-Mn alloy phase, X-ray diffraction (XRD) test was performed. The EDS test was carried out to show the composition at different points and to observe the presence of several phases in the FAMC alloy system. A pin-on-disc method was employed for a dry sliding wear test, and corrosion testing was performed using the three-electrode cell polarization method. With the addition of Mn, the Vickers hardness of the FAMC alloy raised from 194.4 VHN at 15 wt % to 265 VHN at 25 wt %. The tensile strength and fracture elongation values were 424.69 MPa, 27.16 % EI; 434.72 MPa, 33.6 % EI; and 485.71 MPa, 38.48 % EI for FAM15, FAM20, and FAM25, respectively. A crucial factor for increasing the performance of grinding ball is the wear mechanism. The wear rate results for FAM25 show a decline of more than 57 % compared to FAM15 due to an increase in the hard intermetallic area. The addition of Mn elements increased the corrosion resistance of the FAMC alloys; the lowest corrosion rate occurred at 25 wt % Mn content at up to 0.036 mm/yr. According to the experimental results, the FAM25 alloys have the highest mechanical and corrosion resistance of the three types of alloys. The FAMC alloy is a promising candidate for application as a material for grinding balls by optimizing the Mn content

Keywords: Fe-Al-Mn-C, microstructure, mechanical characteristics, wear, impact, corrosion resistance, grinding ball

UDC 621
DOI: 10.15587/1729-4061.2021.225421

DEVELOPMENT OF Fe-5Al-1C ALLOYS FOR GRINDING BALL

Ratna Kartikasari
Doctor of Mechanical Engineering, Associate Professor*
E-mail: ratna@itny.ac.id
Adi Subardi
Doctor of Materials Science and Engineering, Assistance Professor*
E-mail: subardi@itny.ac.id
Andy Erwin Wijaya
Doctor of Mines Engineering, Assistance Professor
Department of Mines Engineering**
E-mail: andyerwin@itny.ac.id
*Department of Mechanical Engineering**
**Institut Teknologi Nasional Yogyakarta
Jl. Babarsari, Caturtunggal, Depok, Sleman, Daerah Istimewa Yogyakarta, Indonesia, 55281

Received date 02.12.2020
Accepted date 01.02.2021
Published date 26.02.2021

1. Introduction

The consumption of domestic cement in Indonesia has increased by 6 % over the past year to 5.33 million tonnes in 2018 as reported by the Indonesian Cement Association. As most of the energy consumed in the Portland cement industry is for clinker milling [1], this presents a major challenge for researchers around the world. In general, the grinding process of raw materials in the manufacture of cement uses a ball mill, and the production cost in ore milling is largely determined by the use of grinding balls. Reducing the total wear mechanism (including abrasion, impact systems, and corrosion) in a ball mill is a significant challenge [2]. Corrosion is the dominant factor to decrease the performance of grinding media due to continuous exposure during grinding [3].

Indonesia still relies on imported grinding balls for use in cement raw material processing such as lime, silicate, alumina, and iron oxide. Nearly half of the world's milling circuits use ball mills, while almost 90 % of the mining operations use balls as grinding devices [4]. Grinding balls are produced from materials with high toughness and hardness properties including Cr, low alloy steel, and white cast iron. Besides, grinding media should be produced to provide the lowest wear rate and greatest efficiency [5]. The Fe-Al-Mn-C system was studied to replace Fe-Cr-Ni-C stainless steels, where Cr and Ni were replaced by less costly Al and Mn [6–8]. Essential parameters of grinding ball quality include size, mass, chemistry, hardness, microstructure, durability, internal stress, and distribution of worn size.

The Fe-Mn-Al-C system is a competitive class of low-density monolithic steels offering a combination of excellent material characteristics (yield strength: 0.4–1.0 GPa, ultimate tensile strength: 0.6–2.0 GPa; elongation: 30–100 %) [9]. Furthermore, as reported, this alloy has several advantages, including high strength and toughness at room and low temperatures [10], high fatigue characteristics [11] and excellent resistance to oxidation at high temperatures [12]. Fe-Mn-Al-C alloys have been described as potential advanced high-strength steels for age hardening and energy absorption in a crash [9]. Investigations on the performance of Fe-Mn-Al-C steels have been widely reported. However, optimization of Mn content in Fe-Mn-Al-C steel systems has not been widely reported.

2. Literature review and problem statement

Until currently, all cement factories in Indonesia still use imported grinding balls as raw material grinders in the cement manufacturing process. The main problem with grinding ball importers made of Fe-Cr alloy is that they are

expensive [8]. Several studies have reported on the use of grinding media for mineral ores [13, 14].

However, the corrosion mechanism's contribution to overall wear is still unreported. The wear mechanism is a critical factor for increasing the efficiency of the grinding ball [15]. It has been shown that the presence of appropriate neutralizer materials such as Mn, Cr, Be, Co and Sr can change the structure of the process to less dangerous forms [16–18]. For instance, Mn is an important factor for the modification of needle-like intermetallic compounds [18–21]. Furthermore, Mn was already widely used to prevent the design of long Fe-rich needle-shaped phases and to facilitate the creation of compact Fe-rich phases in Al alloys [22]. Fe-Mn-Al alloys have received substantial scientific attention in recent decades as a replacement for some of the traditional Fe-Ni-Cr stainless steels. The alloy shows excellent performance, particularly in terms of corrosion resistance and oxidation resistance at high temperatures [23–25]. The preference for Fe-Al-Mn alloys with Al and Mn as a substitute for Cr and Ni used in traditional stainless steels is the main economic and strategic reason for their use [26]. Liu et al. [26] previously reported various isothermal parts of ternary Fe-Mn-Al alloys. These alloys consist of austenite and ferrite phases; some are single phases (austenite or ferrite) and others are double phases. Mn and Al are well-recognized formers of ferrite and austenite, respectively. A higher concentration of Mn results in a higher ratio of the austenite phase emerging at low temperatures compared with the total ferrite phase in low-carbon steels [25]. Sutou and Koster investigated the effect of Mn content on the mechanical behavior of Fe-10Al-1C-Mn [27, 28], and Gassel has reported the properties of Fe-3Si-3Al-Mn alloys [29]. At temperatures above 1.000 °C, all the alloys were solution-treated, followed by water quenching. At room temperature, tensile tests were conducted at strain rates ranging between 1×10^{-4} and 3.3×10^{-4} s^{-1}. Fe-3Si-3Al-Mn and Fe-10Al-1C-Mn alloys exhibited different behavior with Mn addition. Fe-3Si-3Al-Mn and Fe-10Al-1C-Mn alloys showed dissimilar properties with Mn addition. With an increase in the Mn content, Fe-3Si-3Al-Mn alloys showed an increase in ductility followed by a reduction in strength. An interesting study was carried out by Ramos et al (2015) who evaluated the abrasive wear of Fe-29.0Mn-6Al0.9C-1.8Mo-1.6Si-0.4Cu steels [30]. They noticed in this work that during the wear process, the austenite was transformed into martensite. To determine and classify the austenite and martensite material, they used X-ray diffraction and Mössbauer spectroscopy. This transformation has a strong correlation with the increase in sample hardness. This phenomenon has received special attention from researchers because this behavior has not been previously recorded. In the last few decades, great attention of researchers has been focused on improving the performance of Fe-Al-Mn alloys, but the most recommended ratio of Mn content in these alloys has not been reported. Therefore, a new alloy is needed that can replace the Fe-Cr alloy. Among the alloy systems that are most promising to replace Fe-Cr alloys are the superior and economical Fe-Al-Mn alloys [26]. This research will formulate the Mn content ratio, which has a significant effect on the performance of Fe-Al-Mn alloys.

3. The aim and objectives of the study

The aim of the research is to develop Fe-5Al-1C alloys for grinding balls.

To achieve this aim, the following objectives are accomplished:

– to modify the structure of Fe-5Al-1C by adding Mn (15, 20, and 25 %);

– to investigate the mechanical properties (hardness, tensile strength, and impact);

– to investigate the wear and corrosion resistance of Fe-Al-Mn-C alloys.

4. Materials and methods for preparing and testing specimens

The study used a raw material consisting of Fe-C, ferromanganese medium carbon, pure aluminum, and mild steel scrap. The grinding ball composition was manually controlled using the material balance. Patterns of ingot-shaped wood (20×3×3 cm) and ball shapes (diameter of 3 cm) were used in the casting process. Molding sand was used due to the simplicity and cost-effectiveness of the process. Fe-5Al-1C alloy smelting started with the production of starter blocks, which included mild steel scrap, Fe-Mn-C (medium), and Fe-C with a target composition of 1 % C at variations of 15 %, 20 %, and 25 % Mn, respectively. The composition of the three alloys was Fe-5Al-1C-15Mn (FAM15), Fe-5Al-1C-20Mn (FAM20), and Fe-5Al-1C-25Mn (FAM25). Under an Ar atmosphere, the alloys were melted in an induction furnace. Composition control was conducted with a chill tester before pouring, and the molten metal was poured into ball molds and manually ladled into ingot molds. The castings were inspected to ensure that the Fe-Al-Mn alloy samples were free of defects. Specimens were prepared for overall characterization, which included tensile, hardness, impact, and corrosion properties. An X-ray diffraction testing was carried to ensure the Fe-5Al-1C-Mn alloy phase. Tensile test specimens were cut based on the JIS 2201 standard. The Vickers hardness samples were generated on sections of longitudinal ingots. The Charpy impact test specimen measured 3x10x55 mm with a v-notch of 2 mm based on the JIS Z 2242 standard. Corrosion samples were determined by the common practice of ASTM G 30 with 14 mm diameter and 3 mm gauge length.

5. Results of experiment

5. 1. Modification of the Fe-5Al-1C structure

5. 1. 1. Chemical compositions

The XRD patterns for FAM15, FAM20, and FAM25 are shown in Fig. 1. The absence of peaks attributable to impurities indicates that the process of synthesizing the samples was successful. For the FAM15 sample, it is detected that the phase composition is close to both FAM20, and FAM25. Table 1 indicates the chemical compositions of the three specimens.

Chemical composition test to obtain the percentage of chemical elements contained in the specimen. The elements in the Fe-Al-Mn-C alloy greatly affect their mechanical properties. The Mn element in the specimen is expected to replace the properties of the Cr element in the grinding ball alloy, including mechanical properties and corrosion resistance.

The chemical composition of the three specimens was 15.05 % (FAM15), 20.01 % (FAM20), and 25.1 % (FAM25), which showed that they were consistent with the ratio of Mn content applied to these specimens. Furthermore, the Fe element dominates the Fe-Al-C-Mn alloy with a con-

tent of 77.79 % (FAM 15), 72.84 % (FAM20), and 67.77 % (FAM25), respectively.

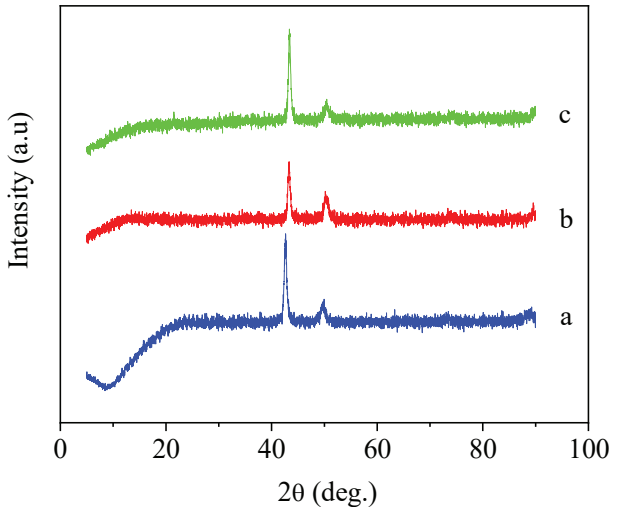

Fig. 1. Curve of room-temperature XRD pattern: *a* — FAM15; *b* — FAM20; *c* — FAM25

Table 1

Chemical alloy composition

Element	FAM15	FAM20	FAM25
Fe	77.79	72.84	67.77
C	1.01	1.02	1.01
Al	5.05	5.03	5.02
Mn	15.05	20.01	25.1
Si	1.05	1.04	1.05
P	0.03	0.02	0.03
S	0.02	0.01	0.02

5. 1. 2. Microstructure of FAMC alloys

Fig. 2, *a* illustrates the microstructure of the FAM15 alloy composed of an austenite matrix with a low ferrite content, which forms a semi-dendritic pattern. It is clear that the presence of Mn as an austenite stabilizer has a dominant effect, whereas the Al element as a stabilizer for ferrite structures has little influence on the formation of ferrite structures.

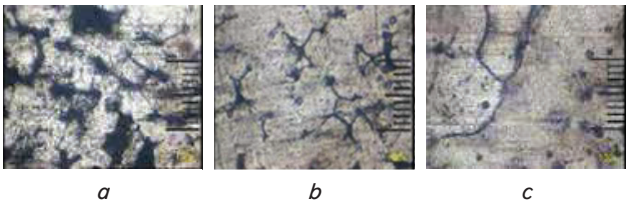

a *b* *c*

Fig. 2. Microstructure: *a* — FAM15; *b* — FAM20; *c* — FAM25

A higher Mn content causes a more dominant austenite structure and a decrease in the ferrite structure. At 25 %, the Mn content in the ferrite structure is not visible as a perfect austenite structure.

5. 2. Mechanical properties

5. 2. 1. Hardness and tensile strength

Hardness is a property that can act as a substitute for a material's strength. The mechanical properties are shown in Fig. 3. The hardness of the three specimens was quite high. As shown in Fig. 3, *a*, the hardness obtained was in the range between 187 VHN (25 % Mn content) to 265 VHN (25 % Mn content). High hardness is the main requirement of grinding ball materials, has a strong correlation with the toughness and resistance of grinding balls.

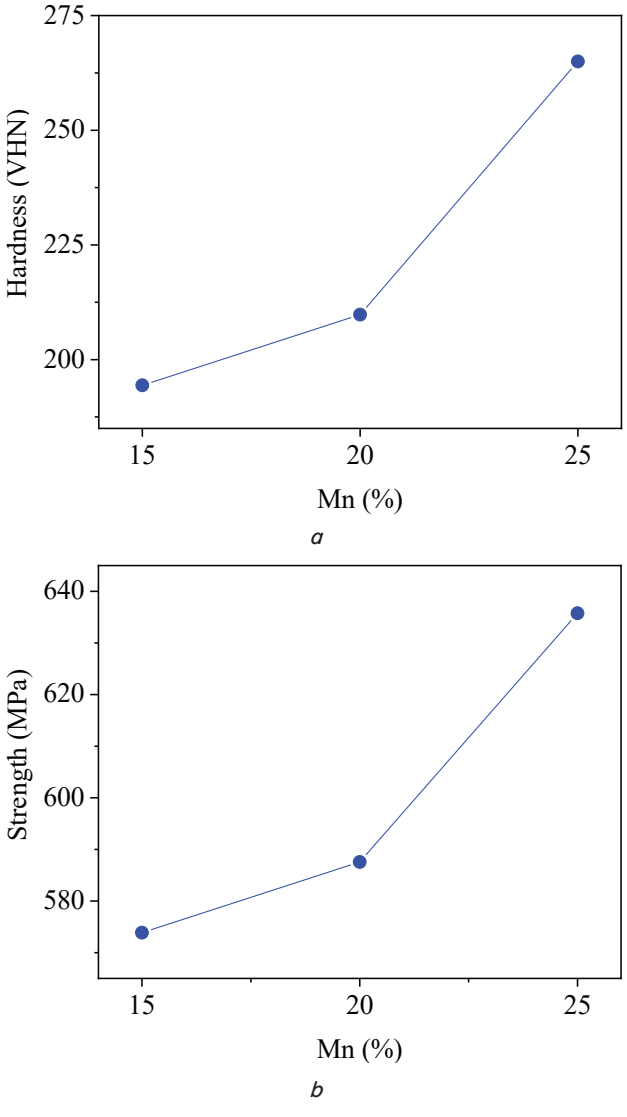

Fig. 3. Mechanical properties curve: *a* — Vickers hardness; *b* — tensile strength of FAM15, FAM20, and FAM25

The figures give the values of the Vickers hardness test, the tensile strength, and proportion elongation as a function of the Mn addition ratio. The variation of the Vickers hardness value with the volume percentage of Mn in the Fe-5Al-1C alloy is shown in Fig. 3, *a*.

Table 2 shows the FAMC alloy tensile strength values are within the range of 573.86–635.76 MPa, where a higher Mn content provides higher tensile resistance. These data indicate that the ratio of Mn content has a significant impact on the tensile strength of the specimen.

The same phenomenon as tensile strength, the yield strength value of the specimen increases with increasing Mn content in the Fe-Al-C-Mn alloy. As shown in Table 2, the yield strength values are in the range between 424.69 and 485.71 MPa. The specimens' tensile behavior is shown in Fig. 3, *b*. The FAMC alloy has a strain of 27.16 with 15 % Mn.

The strain increased to 33.6 % and 38.48 %, respectively, for specimens with 20 % Mn and 25 % Mn. The higher strain present in the higher Mn is due to lower lattice density at higher Mn. This is the effect of the Mn atom, which occupies the position of the Fe atom is greater than the Fe atom.

Table 2

Fe-Al-Mn alloy tensile test

Fe-Al-C alloys (% Mn)	Tensile strength (MPa)	Yield strength (MPa)	Strain (%)
15 (FAM15)	573.86	424.69	27.16
20 (FAM20)	587.56	434.72	33.60
25 (FAM25)	635.76	485.71	38.48

Fig. 4 shows the fracture surfaces of the three specimens after the tensile test. The FAM25 specimen (Fig. 4, *c*) shows a reduction in cross-section resulting in a fracture. The increase in Mn content up to 25 % has an impact on the ductility of the specimen.

From the tensile test data, the tensile strength values of the three specimens were obtained (FAM15, FAM20, FAM25). While the microstructure is generated data in the form of a fracture surface image using the SEM. The process of taking microstructure images is that the specimen is placed on a precision table, the specimen is set to get the expected image, so the results can be seen in Fig. 4.

Fig. 5, 6 show the phenomenon that can be observed from the EDS test data, which shows different compositions at different points and reveals the presence of several phases in the Fe-A-Mn alloy system.

Overall, Fig. 5, 6 show that the alloying elements of the specimens were consistent with the element ratio calculations applied when specimen manufacturing. Specimen elements are detected in the Fe-Al-Mn alloy system.

a *b* *c*

Fig. 4. SEM micrographs of fracture surface after the tensile test: *a* — FAM15; *b* — FAM20; *c* — FAM25

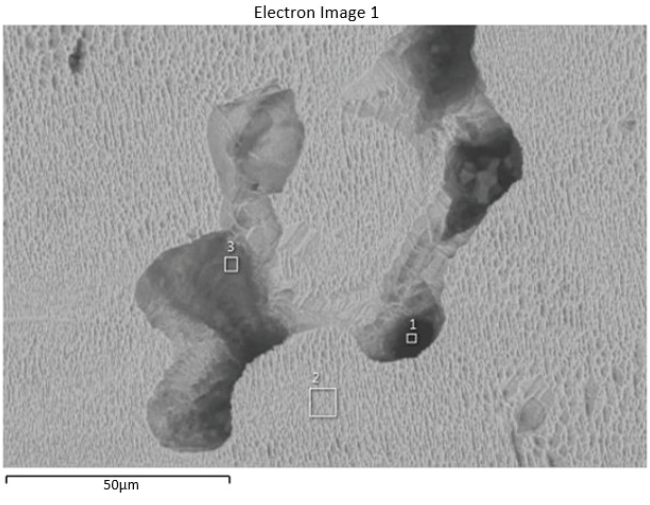

Fig. 5. SEM micrograph: FAM25

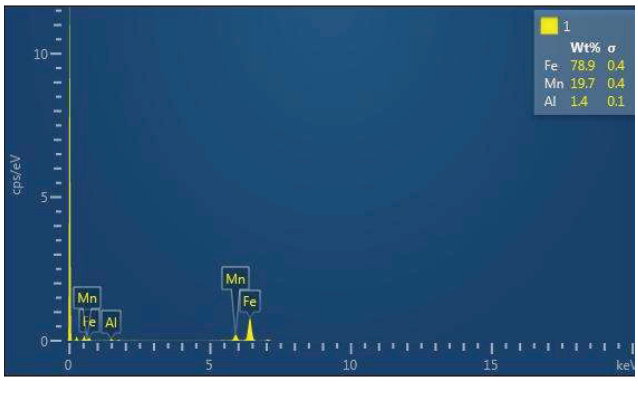

a

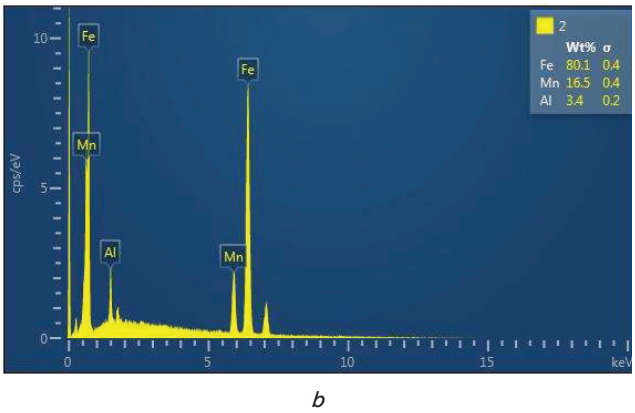

b

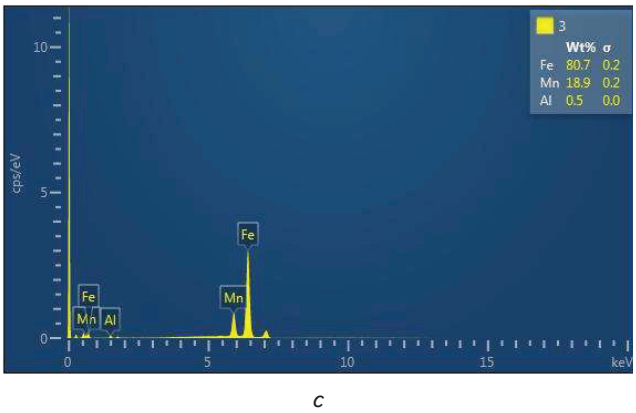

c

Fig. 6. EDS spectra referring to intermetallic phases labeled: *a* — 1; *b* — 2; *c* — 3

5. 2. 2. Impact properties

Fig. 7 shows the impact (toughness) effect on the Mn content for the FAM alloys. Impact testing was conducted using the Charpy method, and the specimen standard refers to ASTM E 23 type A. The specimen reveals that the toughness value increases with rising contents of Mn (%).

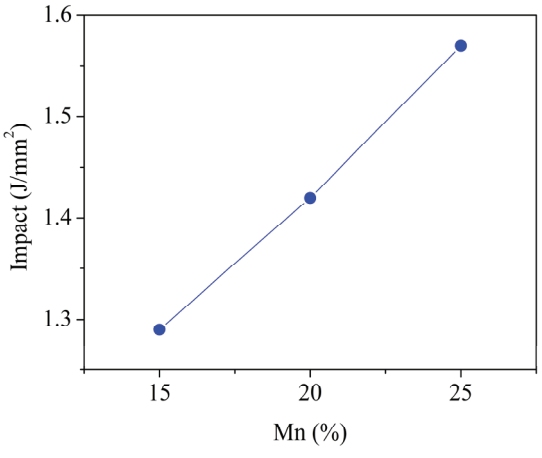

Fig. 7. Effect of Mn content on impact for the Fe-Al alloy

Impact testing is performed to measure the resistance of a material to shock loads. Impact testing simulates the operating conditions of a material based on working conditions. From Fig. 7, the toughness value of the specimen increases sharply with the addition of up to 25 % Mn. The high toughness of grinding ball materials has a strong correlation to the overall performance of grinding balls in the cement industry.

5. 3. Physical properties

5. 3. 1. Wear properties

The wear is proportional to the surface area and increases with the quantity of exposed surface area. Fig. 8 shows the impacts of Mn on the base alloy wear rate. It is evident that adding Mn elements to the Fe-Al-C alloy affects the wear rate significantly. The lowest wear was obtained by the FAM15 specimen (15 % Mn content) and the highest wear occurred on the FAM 25 specimen (25 % Mn content).

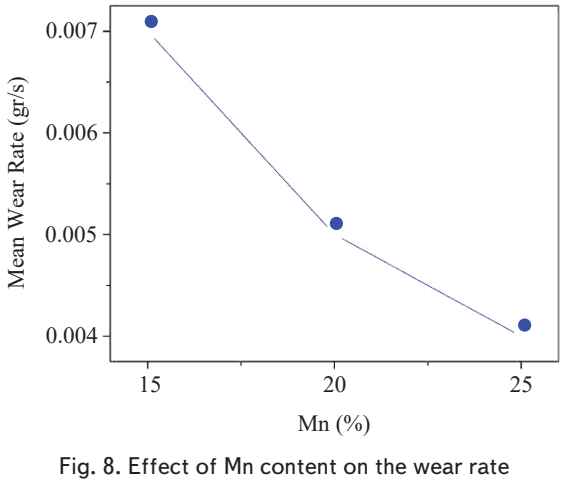

Fig. 8. Effect of Mn content on the wear rate

Microstructural changes occur within the range of increasing Mn content, and the ferrite structure decreases as Mn content increases. This is accompanied by an increase in the area of the formed austenite structure, which results in improved wear resistance.

5. 3. 2. Corrosion resistance

Fig. 9 shows the effect of Mn content on corrosion behavior. Corrosion testing was conducted by calculating the corrosion rate of the samples using the weight difference before and after soaking in a 0.5 % HCl (chloride acid) solution. This confirms that adding Mn elements can increase the corrosion resistance of FAMC alloys.

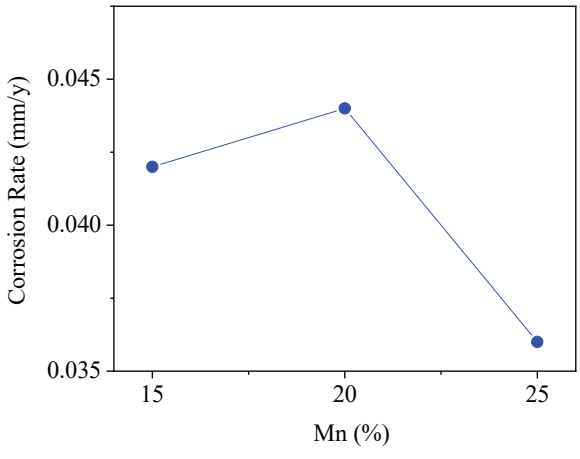

Fig. 9. Corrosion rate curve for FAM15, FAM20, and FAM25

Corrosion is a major cause of material failure (construction) and gets great attention from designers in material selection. The addition of the Mn element in the Fe-Cr alloy has shown a significant impact in reducing the corrosion rate of grinding ball materials. These results are consistent with the studies that have been previously reported.

6. Discussion of experimental results

For chemical analyses as shown in Table 1, the data revealed that the FAM15, FAM20, and FAM25 samples were FAMC high-alloy steel, which contains carbon, aluminum, manganese, silicon, phosphorus, and sulfur elements. The Mn element in the aluminum alloy can prevent precipitation so that it is more resistant to attack by corrosion. The proportion of the alloy applied affects the microstructure, the grain size, and metal alloy mechanical strength. The other elements are referred to as impurities and do not affect the alloy metal's properties.

To describe the microstructure more deeply, the SEM was used to observe the three specimens. The FAM15 (Fig. 2, *a*) and FAM20 (Fig. 2, *b*) specimens form a temporary duplex, while the FAM25 sample (Fig. 2, *c*) is an austenitic structure. At 5 % Mn content, a double phase in the FAM15 and FAM20 samples due to the Al content appears, and the alloy phase is 100 % ferritic at an Al content above 10 % [31]. The Mn content is still classified as low to medium and has not been able to convert ferritic structures to perfect austenite. The contribution of 5–10 % Mn to the Fe-Al-C alloy structure forms a duplex α/γ [32].

The Vickers hardness of the Fe-5Al-1C alloy specimen is improved by adding Mn; this phenomenon is similar to that reported previously [26]. The rise in Mn content from 15 % to 20 % resulted in a rise in the hardness of 7.9 %, the hardness value increased up to 36.3 % at 25 % Mn content. The maximum hardness value was achieved at 25 % Mn content (265 VHN). When modifications to the microstructure were identified within the range of increasing Mn content,

the ferrite structure was also seen to decrease with a rise in Mn content; this was accompanied by an increase in the amount of austenite structure that was formed, which also caused the hardness value to increase. Since the Mn atom (1.79 Å) is smaller than the Al atom (1.82 Å) and is similar to the Fe atom (1.72 Å), the improvement in the hardness value is quite large.

The FAMC alloys yield strength ranges between 424.69 and 485.71 MPa, while the strain values range from 27.16 % to 38.48 %. After the hardness test, the fracture surfaces of the samples display a brittle and ductile combined fracture pattern (Fig. 4), this means that the FAMC alloy has quite a high toughness value. As previously studied, Mn in steel plays a role in increasing strength [33]; this study verified that a higher Mn content leads to higher tensile strength and yield in this alloy.

The strength increase followed by strain improvement is an advantage of the FAMC alloy. The combined impact of the elements (Al, Mn, and C) presence in the alloy system facilitates the process. The structure of FAMC solid leads to a significant and simultaneous improvement in strength and strain. The result is consistent with the previously reported investigations in which the presence of 2 wt% Mn in the Fe-10.5Al-0.7C alloy system increases the tensile strength value to 8.25 % and 44.4 % strain [32]. Furthermore, the maximum wear value is 15 % at the lowest Mn content; increased the Mn content, the reduced the wear value. A raised Mn content lowers the wear value by up to 28.6 % at 20 % Mn and up to 42.9 % at 25 % Mn.

In the Fe-Al-C alloy system, an addition of 20 wt% Mn resulted in an increasing trend in toughness up to 1.42 J/mm^2. Specimen by 25 wt % Mn content, the toughness continued to increase to the highest value of 1.57 J/mm^2. Therefore, it can be assumed that Mn has enhanced mechanical properties in the Fe-Al-C alloy. This is because manganese neutralizes the element that can change morphology in the β-phase [20, 21].

Adding Mn to Fe-Al-C alloys increases the corrosion resistance, strength, and toughness of the metal alloys [34]. The lowest corrosion rate of the FAMC alloys occurred at a 25 wt % Mn content at up to 0.036 mm/yr. The FAMC alloy has a 0.036–0.042 mm/yr corrosion rate in 0.5 % NaCl; there is a tendency for the corrosion rate to decrease in alloys with a higher Mn content. The Mn element in the alloy improves both strength and toughness; it also contributes to sustaining the austenite formation at room temperature and improves the corrosion protection of alloy metals. According to the overall results, the corrosion resistance of 25 % Mn FAMC alloys is in the acceptable range. A raised Mn content increases the corrosion resistance up to 14.2 %.

In general, this study is limited to mechanical and physical properties and has not investigated the fatigue properties of Fe-Al-Mn-C alloy steels. Fatigue testing can describe the performance of the material under actual working conditions. However, the hardness and tensile strength tests can reflect the properties of alloy steels including fatigue properties. Besides, the improved performance of the Fe-Al-Mn-C steel alloys requires further development. Simple methods can be applied through heat treatment including age hardening and surface hardening. This method can increase hardness, ductility, and wear resistance.

7. Conclusions

1. The structure of the Fe-Al-C alloy into Fe-Al-Mn-C has been successfully developed by the addition of Mn. The main elements contained in the sample are Fe, Al, Mn, and C. The proportion of alloy elements applied affects the microstructure, grain size and mechanical properties and physical properties of the alloy steel.

2. The microstructure of the specimens is categorized as a temporary duplex (FAM15 and FAM20), and an austenitic structure (FAM25). The maximum hardness value is 265 VHN (FAM25 specimen) with the addition of 25 % Mn. The structure of the FAMC alloy shows a significant and simultaneous increase in strength and strain. The toughness of the specimens increased with increasing Mn contents, the maximum toughness value was 1.57 J/mm^2. The lowest corrosion rate is 0.036 mm/yr recorded by specimens with 25 % Mn content.

Acknowledgments

The study was funded by the Ministry of Research, Technology and Higher Education of the Indonesia Republic "National Institution Research Grant-STRANAS" under Decree number: 3/E/KPT/'18 and Research Contract number: 04.c/STTNAS/P3M/Pen.DRPM/III/'18.

References

1. Jankovic, A., Valery, W., Davis, E. (2004). Cement grinding optimisation. Minerals Engineering, 17 (11-12), 1075–1081. doi: https://doi.org/10.1016/j.mineng.2004.06.031
2. Iwasaki, I., Riemer, S. C., Orlich, J. N., Natarajan, K. A. (1985). Corrosive and abrasive wear in ore grinding. Wear, 103 (3), 253–267. doi: https://doi.org/10.1016/0043-1648(85)90014-6
3. Jang, J. W., Iwasaki, I., Moore, J. J. (1989). The Effect of Galvanic Interaction Between Martensite and Ferrite in Grinding Media Wear. CORROSION, 45 (5), 402–407. doi: https://doi.org/10.5006/1.3582036
4. Wei, D., Craig, I. K. (2009). Grinding mill circuits – A survey of control and economic concerns. International Journal of Mineral Processing, 90 (1-4), 56–66. doi: https://doi.org/10.1016/j.minpro.2008.10.009
5. Jankovic, A., Wills, T., Dikmen, S. (2016). A comparison of wear rates of ball mill grinding media. Journal of Mining and Metallurgy A: Mining, 52 (1), 1–10. doi: https://doi.org/10.5937/jmma1601001j
6. Lai, H. J., Wan, C. M. (1989). The study of work hardening in Fe-Mn-Al-C alloys. Journal of Materials Science, 24 (7), 2449–2453. doi: https://doi.org/10.1007/bf01174510
7. Chen, F. C., Li, P., Chu, S. L., Chou, C. P. (1991). Evidence of strain-induced martensitic transformation in Fe-Mn-Al austenitic alloy steels at room temperature. Scripta Metallurgica et Materialia, 25 (3), 585–590. doi: https://doi.org/10.1016/0956-716x(91)90096-j
8. Kim, Y. G., Han, J. M., Lee, J. S. (1989). Composition and temperature dependence of tensile properties of austenitic Fe-Mn-Al-C alloys. Materials Science and Engineering: A, 114, 51–59. doi: https://doi.org/10.1016/0921-5093(89)90844-7

9. Frommeyer, G., Brüx, U. (2006). Microstructures and Mechanical Properties of High-Strength Fe-Mn-Al-C Light-Weight TRIPLEX Steels. Steel Research International, 77 (9-10), 627–633. doi: https://doi.org/10.1002/srin.200606440
10. Kim, Y. G., Park, Y. S., Han, J. K. (1985). Low temperature mechanical behavior of microalloyed and controlled-rolled Fe-Mn-Al-C-X alloys. Metallurgical Transactions A, 16 (9), 1689–1693. doi: https://doi.org/10.1007/bf02663026
11. Kalashnikov, I. S., Acselrad, O., Kalichak, T., Khadyyev, M. S., Pereira, L. C. (2000). Behavior of Fe-Mn-Al-C Steels during Cyclic Tests. Journal of Materials Engineering and Performance, 9 (3), 334–337. doi: https://doi.org/10.1361/105994900770346015
12. Kao, C. H., Wan, C. M. (1988). Effect of temperature on the oxidation of Fe-7.5A1-o.65C alloy. Journal of Materials Science, 23 (6), 1943–1947. doi: https://doi.org/10.1007/bf01115754
13. Natarajan, K. A. (1996). Laboratory studies on ball wear in the grinding of a chalcopyrite ore. International Journal of Mineral Processing, 46 (3-4), 205–213. doi: https://doi.org/10.1016/0301-7516(95)00093-3
14. Chenje, T. W., Simbi, D. J., Navara, E. (2003). The role of corrosive wear during laboratory milling. Minerals Engineering, 16 (7), 619–624. doi: https://doi.org/10.1016/s0892-6875(03)00132-8
15. Massola, C. P., Chaves, A. P., Albertin, E. (2016). A discussion on the measurement of grinding media wear. Journal of Materials Research and Technology, 5 (3), 282–288. doi: https://doi.org/10.1016/j.jmrt.2015.12.003
16. Gupta, S. P. (2002). Intermetallic compound formation in Fe–Al–Si ternary system: Part I. Materials Characterization, 49 (4), 269–291. doi: https://doi.org/10.1016/s1044-5803(03)00006-8
17. Harun, M., Talib, I. A., Daud, A. R. (1996). Effect of element additions on wear property of eutectic aluminium-silicon alloys. Wear, 194 (1-2), 54–59. doi: https://doi.org/10.1016/0043-1648(95)06707-8
18. Bidmeshki, C., Abouei, V., Saghafian, H., Shabestari, S. G., Noghani, M. T. (2016). Effect of Mn addition on Fe-rich intermetallics morphology and dry sliding wear investigation of hypereutectic Al-17.5%Si alloys. Journal of Materials Research and Technology, 5 (3), 250–258. doi: https://doi.org/10.1016/j.jmrt.2015.11.008
19. Murali, S., Raman, K. S., Murthy, K. S. S. (1995). The formation of β-$FeSiAl_5$ and Be-Fe phases in Al-7Si-0.3Mg alloy containing Be. Materials Science and Engineering: A, 190 (1-2), 165–172. doi: https://doi.org/10.1016/0921-5093(94)09602-s
20. Mulazimoglu, M. H., Zaluska, A., Gruzleski, J. E., Paray, F. (1996). Electron microscope study of Al-Fe-Si intermetallics in 6201 aluminum alloy. Metallurgical and Materials Transactions A, 27 (4), 929–936. doi: https://doi.org/10.1007/bf02649760
21. Shabestari, S. G., Mahmudi, M., Emamy, M., Campbell, J. (2002). Effect of Mn and Sr on intermetallics in Fe-rich eutectic Al-Si alloy. International Journal of Cast Metals Research, 15 (1), 17–24. doi: https://doi.org/10.1080/13640461.2002.11819459
22. Ji, S., Yang, W., Gao, F., Watson, D., Fan, Z. (2013). Effect of iron on the microstructure and mechanical property of Al–Mg–Si–Mn and Al–Mg–Si diecast alloys. Materials Science and Engineering: A, 564, 130–139. doi: https://doi.org/10.1016/j.msea.2012.11.095
23. Jackson, P. R. S., Wallwork, G. R. (1984). High temperature oxidation of iron-manganese-aluminum based alloys. Oxidation of Metals, 21 (3-4), 135–170. doi: https://doi.org/10.1007/bf00741468
24. Duh, J. G., Wang, C. J. (1990). Formation and growth morphology of oxidation-induced ferrite layer in Fe-Mn-Al-Cr-C alloys. Journal of Materials Science, 25 (4), 2063–2070. doi: https://doi.org/10.1007/bf01045765
25. Liu, X. J., Hao, S. M., Xu, L. Y., Guo, Y. F., Chen, H. (1996). Experimental study of the phase equilibria in the Fe-Mn-Al system. Metallurgical and Materials Transactions A, 27 (9), 2429–2435. doi: https://doi.org/10.1007/bf02652336
26. Cheng, W.-C., Liu, C.-F., Lai, Y.-F. (2002). Observing the D03 phase in Fe–Mn–Al alloys. Materials Science and Engineering: A, 337 (1-2), 281–286. doi: https://doi.org/10.1016/s0921-5093(02)00047-3
27. Sutou, Y., Kamiya, N., Umino, R., Ohnuma, I., Ishida, K. (2010). High-strength Fe–20Mn–Al–C-based Alloys with Low Density. ISIJ International, 50 (6), 893–899. doi: https://doi.org/10.2355/isijinternational.50.893
28. Chang, S. C., Hsiau, Y. H., Jahn, M. T. (1989). Tensile and fatigue properties of Fe-Mn-Al-C alloys. Journal of Materials Science, 24 (3), 1117–1120. doi: https://doi.org/10.1007/bf01148807
29. Grässel, O., Krüger, L., Frommeyer, G., Meyer, L. W. (2000). High strength Fe–Mn–(Al, Si) TRIP/TWIP steels development – properties – application. International Journal of Plasticity, 16(10-11), 1391–1409. doi: https://doi.org/10.1016/s0749-6419(00)00015-2
30. Hua, D., Huaying, L., Zhiqiang, W., Mingli, H., Haoze, L., Qibin, X. (2013). Microstructural Evolution and Deformation Behaviors of Fe-Mn-Al-C Steels with Different Stacking Fault Energies. Steel Research International, 84 (12), 1288–1293. doi: https://doi.org/10.1002/srin.201300052
31. Baligidad, R. G., Prasad, V. V. S., Rao, A. S. (2007). Effect of Ti, W, Mn, Mo and Si on microstructure and mechanical properties of high carbon Fe–10·5 wt-%Al alloy. Materials Science and Technology, 23 (5), 613–619. doi: https://doi.org/10.1179/174328407x158631
32. Kim, H., Suh, D.-W., Kim, N. J. (2013). Fe–Al–Mn–C lightweight structural alloys: a review on the microstructures and mechanical properties. Science and Technology of Advanced Materials, 14(1), 014205. doi: https://doi.org/10.1088/1468-6996/14/1/014205
33. Zuidema, B. K., Subramanyam, D. K., Leslie, W. C. (1987). The effect of aluminum on the work hardening and wear resistance of hadfield manganese steel. Metallurgical Transactions A, 18 (9), 1629–1639. doi: https://doi.org/10.1007/bf02646146
34. Baligidad, R. G., Prasad, K. S. (2007). Effect of Al and C on structure and mechanical properties of Fe–Al–C alloys. Materials Science and Technology, 23 (1), 38–44. doi: https://doi.org/10.1179/174328407x158389